

# A Case Study of Multi-resolution Representation of Heads

Jianwei Niu<sup>1</sup>, Zhizhong Li<sup>1</sup>, and Gavriel Salvendy<sup>1,2</sup>

<sup>1</sup>Department of Industrial Engineering, Tsinghua University, Beijing, 100084, China

<sup>2</sup>School of Industrial Engineering, Purdue University, West Lafayette, IN.,

47907, USA

zzli@tsinghua.edu.cn

**Abstract.** A wavelet analysis based multi-resolution representation method is adopted to establish mathematical description of three-dimensional anthropometric head data in this paper. This method provides flexible description of shapes at different resolution levels. Three-dimensional anthropometric data analysis can then be performed with coarse resolutions, which preserve the major shape components but ignore micro shape components. In a case study of 510 3D head scans, quantitative approximation errors, which reflect the approximation of the low-resolution surface to the original one, have been investigated and demonstrated with respect to various decomposition levels.

**Keywords:** 3D Anthropometry, wavelet analysis, multi-resolution representation.

## 1 Introduction

In the area of population grouping and human accommodation, many attempts have been made to measure and categorize the scope of human body variation [1, 2, 3]. However, geometric characteristics and internal structure of human surface points are not adequately considered in traditional univariate and bivariate methods [4]. This leads to design deficiency on fitting comfort. It is necessary to understand and characterize the range of human body shape variation using three-dimensional (3D) anthropometric data, since it would strongly support better product and workspace design.

In recent years, several large 3D anthropometric surveys have been conducted [5, 6, 7, 8]. The 3D human body data can have wide application in industry, such as design of shoes [9] and spectacle frames [10], apparel design [11, 3], and helmet evaluation [1, 2]. Unfortunately, there are two great problems in data analysis for 3D scanning anthropometry, i.e., the computational load and enormous storage memory. People look forward to the balance between the conflicting requirements of low data size and high accuracy [12, 13]. One way is to find a method enabling data manipulation and analysis progressively in a coarse-to-fine fashion. Multi-resolution analysis, e.g., wavelet-based analysis, provides such a useful and efficient tool for representing shape and analyzing features at multiple levels of detail and is rapidly becoming an attractive technique in 3D computer graphics and 3D geometric modelling [14, 15]. Wavelet analysis can produce a multi-resolution pyramid representation of the original data. In

the wavelet domain, it is easier to manipulate shape features at different scales and analyze data on different resolutions. In this paper a multi-resolution description of human head shape based on wavelet decomposition is introduced. We restrict our attention to the case of cubic B-splines defined on a knot sequence that is uniformly spaced everywhere except at its ends, where its knots have multiplicity of 4. Such B-splines are commonly referred to as endpoint-interpolating cubic B-splines [16]. Approximation errors under different resolutions are illustrated in a case study of 510 head samples.

This paper is organized as follows. Section 2 introduces fundamentals of B-spline wavelets. Section 3 presents the detail procedure of wavelet transformation of 3D anthropometric data. A case study of multi-resolution description of 3D head data is then presented in section 4. Conclusions are given in section 5.

## 2 Fundamentals of B-Spline Wavelets

For any integer  $j \geq 0$ , let  $V^j$  be the space spanned by the endpoint-interpolating B-spline basis functions of degree 3 with  $2^j$  uniform intervals in domain  $[0, 1]$ . In other words, for any  $f(x)$  in  $V^j$ ,  $f(x)$  is a polynomial spline function of degree 3 with continuous second derivative and the knot vector defining the function is  $(0, 0, 0, 0, 1/2^j, 2/2^j, \dots, 1 - 1/2^j, 1, 1, 1, 1)$ . Since  $f(x)$  is also in  $V^{j+1}$ ,  $V^j < V^{j+1}$  holds. The B-spline basis functions in  $V_j$  are called scaling functions and the integer  $j$  is called resolution level. In this research, the cubic endpoint-interpolating B-spline functions defined on a closed interval are of interest in particular. These functions are discussed in detail in many texts on computer-aided design [17, 18, 19].

For any  $f(x)$  and  $g(x)$  in  $V^j$ , we define their inner product. For each  $j$ , we can define  $W_j$  as the space that consists of all functions in  $V_{j+1}$  that are orthogonal to all functions in  $V_j$  under the chosen inner product. The  $2^j$  basis functions of  $W_j$  are so-called endpoint-interpolating cubic B-spline wavelets [20]. For any resolution level  $j$  and any B-spline function  $f_{j+1}$  in  $V_{j+1}$ ,  $f_{j+1}$  can be represented uniquely by the sum of function  $f_j$  in  $V_j$  and function  $g_j$  in  $W_j$  [16]. Such decomposing procedure can be applied recursively to the new spline function  $f_j$ . Wavelets can be used to represent parametric curves and surfaces simply by computing the wavelet decomposition of each coordinate function, separately [16].

## 3 Wavelet Analysis of 3D Surface

It's well known that endpoint-interpolating cubic B-spline wavelets defined on a closed interval is one of the important wavelets used in MRA of curves and surfaces [16, 20]. If not specially mentioned, we will regard them as default wavelets in our paper.

### 3.1 Transformation from Arbitrary Bi-cubic to Quasi-uniform B-Spline Surfaces

In order to ensure high computation efficiency in calculating the control knots, semi-uniform B-Spline surface will be used, since its wavelets base on constant

coefficient matrices, which results in no need to calculate the base each time when calculating the control knots of the surface on each decomposition level [16, 20].

Let  $S(u, v)$  ( $0 \leq u, v \leq 1$ ) be arbitrary B-spline surface defined by  $m$  control points and knot vector  $(u_0, u_0, u_0, u_0, \dots, u_{m-4}, u_{m-3}, u_{m-3}, u_{m-3}, u_{m-3})$  in  $u$  direction, and  $n$  control points and knot vector  $(v_0, v_0, v_0, v_0, \dots, v_{n-4}, v_{n-3}, v_{n-3}, v_{n-3}, v_{n-3})$  in  $v$  direction. Elements of each knot vector correspond to the parametric knots in  $u, v$  direction respectively where the interpolation takes place. Due that we adopt accumulated chord length parameterization, we choose  $u_0 = v_0 = 0, u_{n-3} = v_{n-3} = 1$ . Then select two integers  $j_1 > 0$  and  $j_2 > 0$  which satisfy  $m \leq 2^{j_1} + 3, n \leq 2^{j_2} + 3$ . Calculate the data points  $S(k/2^{j_1}, l/2^{j_2})$  ( $k = 0, 1, \dots, 2^{j_1}, l = 0, 1, \dots, 2^{j_2}$ ) for each  $(u, v) = (k/2^{j_1}, l/2^{j_2})$ . From the  $(2^{j_1} + 1) \times (2^{j_2} + 1)$  data points  $S(k/2^{j_1}, l/2^{j_2})$ , together with additional boundary conditions, the generation of a quasi uniform B-spline surface  $S_{j_1, j_2}(u, v)$  with  $(2^{j_1} + 3) \times (2^{j_2} + 3)$  control points can be implemented by interpolation in  $U$  direction and then interpolation in  $V$  direction. Finally, we obtain quasi-uniform cubic B-spline surface of the original one.

### 3.2 Wavelet Decomposition of Quasi-uniform Cubic B-Spline Curves

For any integer  $j \geq 0$ , let  $B_0^{(j)}, B_1^{(j)}, \dots, B_{2^j+2}^{(j)}$  be cubic B-spline basis functions

defined by knots vector  $(0, 0, 0, 0, 1/2^j, 2/2^j, \dots, 1-1/2^j, 1, 1, 1)$ , and  $V^j$  be the linear space spanned by the  $2^j+3$  basis functions. Let the basis functions of  $V^{j-1}$  and  $V^j$  denoted by  $B_k^{(j-1)}$  ( $k=0,1,\dots,2^{j-1}+2$ ) and  $B_l^{(j)}$  ( $l=0,1,\dots,2^j+2$ ) respectively. From the recursive formula of DeBoor [21], each basis function of  $V^{j-1}$  could be expressed by linear combination of basis functions of  $V^j$ . According to linear algebra theorem [22], there exists one and only one orthogonal complement of  $V^{j-1}$  in  $V^j$  under the presupposition of standard inner product, denoted by  $W^{j-1}$ . Let the basis functions vectors of  $V^j, W^j$  denoted by  $\Phi_j, \Psi_j$  respectively.

For any quasi-uniform cubic B-spline curve  $\gamma(t) = (x(t), y(t), z(t))$  ( $0 \leq t \leq 1$ ) with  $2^j + 3$  control points, where  $x(t), y(t)$ , and  $z(t)$  are in  $V^j$ , and  $j$  is a non-negative integer,

$$\gamma_j(t) = \Phi_j C_j \tag{1}$$

where  $C_j$  is the  $i$ th column vector composed of the control points. Assuming  $\Phi_j$  given, the curve  $\gamma_j(t)$  corresponds to the control points sequence  $C_j$  uniquely.

If wavelet decomposition is implemented in each coordinate of  $\gamma_j(t)$ , the decomposition process of  $\gamma_j(t)$  can be regarded as solving the linear system of [20]

$$C_j = P_j C_{j-1} + Q_j D_{j-1} = \begin{bmatrix} P_j & Q_j \end{bmatrix} \begin{bmatrix} C_{j-1} \\ D_{j-1} \end{bmatrix} \tag{2}$$

where  $\begin{bmatrix} P_j & Q_j \end{bmatrix}$  denotes a block matrix with left part  $[P_j]$  and right part  $[Q_j]$ , and

$\begin{bmatrix} C_{j-1} \\ D_{j-1} \end{bmatrix}$  denotes a block matrix with upper part  $[C_{j-1}]$  and nether part  $[D_{j-1}]$ . In this

way,  $C_j$  can be decomposed into a low-resolution part  $C_{j-1}$  and a detail part  $D_{j-1}$ , which is equivalent to decomposing  $\gamma_j(t)$  into a low-resolution part  $\Phi_{j-1}C_{j-1}$  and a detail part  $\Psi_{j-1}D_{j-1}$ .

### 3.3 Wavelet Decomposition of Quasi-uniform Bi-cubic B-Spline Surfaces

Let  $S_{j_1, j_2}(u, v)$  ( $0 \leq u, v \leq 1$ ) be a bi-cubic quasi-uniform B-spline surface defined by  $m$  scaling functions in  $V_{j_1}$ ,  $n$  scaling functions in  $V_{j_2}$ , and  $m \times n$  control points  $P_{i, k}$  ( $0 \leq i < m, 0 \leq k < n$ ), where

$$m = 2^{j_1} + 3, n = 2^{j_2} + 3. \tag{3}$$

Then

$$S_{j_1, j_2}(u, v) = \Phi_{j_1}(u)P \begin{bmatrix} \Phi_{j_2}(v) \end{bmatrix}^T. \tag{4}$$

where  $\Phi_{j_1}$  and  $\Phi_{j_2}$  are row vectors consisting of scaling functions in  $V_{j_1}$  and  $V_{j_2}$ , respectively.  $P$  is an  $m \times n$  matrix generated from control points  $P_{i, k}$  ( $0 \leq i < m, 0 \leq k < n$ ). Using the algorithm introduced by Quak & Weyrich [23], we obtain

$$S_{j_1, j_2}(u, v) = S_{j_1-1, j_2-1}(u, v) + T_{j_1-1, j_2-1}(u, v). \tag{5}$$

where

$$S_{j_1-1, j_2-1}(u, v) = \Phi_{j_1-1}(u)(A_{j_1} P A_{j_2}^T) \Phi_{j_2-1}^T(v). \tag{6}$$

is a bi-cubic quasi-uniform B-spline surface with  $(2^{j_1-1}+3) \times (2^{j_2-1}+3)$  control points and regarded as the low resolution part of the original surface  $S_{j_1, j_2}(u, v)$ .

## 4 Preliminary Analysis of 3D Head Data

510 head samples have been analyzed. Approximation errors under different resolutions are illustrated. In Fig. 1, surfaces (a), (b), (c) and (d) correspond to the original surface and the decomposed surfaces at the first, third and fifth levels, defined by 12468, 4489, 361 and 49 control points, respectively. It can be seen that the decomposed surface can describe the main shape of the original form.

Distances between the original surface and the low-resolution surface can help to evaluate the approximation error of the decomposition. Let  $V$  be the set of  $(u_k, v_l)$  ( $k=0,1,\dots,m-3; l=0,1,\dots,n-3$ ),  $P(u, v)$  be the data point at the knot of  $(u_k, v_l)$  on original surface  $S(u, v)$  and let  $S'$  be the new surface, then we introduce the idea of

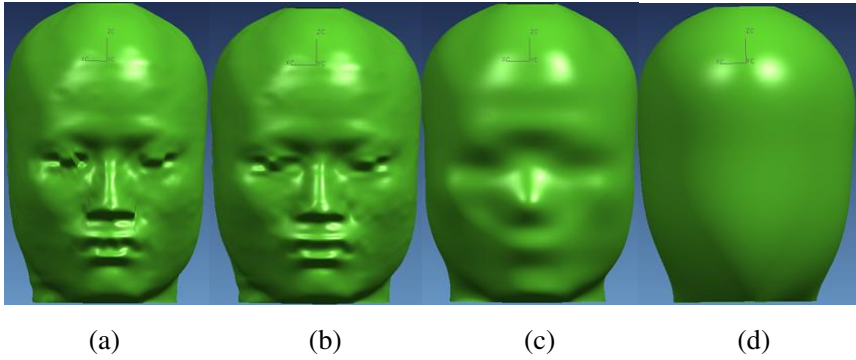


**Fig. 1.** Multi-resolution modeling of an arbitrary bi-cubic surface

Averaged Distance ( $AD$ ) between the original surface and the new surface.  $AD$  can be defined as

$$AD = \underset{(u,v) \in V}{\text{average}} \left| P(u, v) - S' \right| \quad (7)$$

Averaged Relative Error ( $AvgRE$ ) can be defined as

$$AvgRE = \frac{AD}{\max_{(x,y,z) \in (u,v)} (\max(x) - \min(x), \max(y) - \min(y), \max(z) - \min(z))} \quad (8)$$

**Table 1.** Decomposition results of one sample

surface	decomposition level	$MD$ (mm)	$MaxRE$ (%)	$AD$ (mm)	$AvgRE$ (%)	control points number
$S_{6,6}(u, v)$	1	1.813	0.788	0.109	0.047	$(2^6 + 3) * (2^6 + 3) = 4489$
$S_{5,5}(u, v)$	2	2.754	1.198	0.169	0.073	$(2^5 + 3) * (2^5 + 3) = 1225$
$S_{4,4}(u, v)$	3	5.696	2.477	0.447	0.194	$(2^4 + 3) * (2^4 + 3) = 361$
$S_{3,3}(u, v)$	4	13.899	6.043	1.078	0.469	$(2^3 + 3) * (2^3 + 3) = 121$
$S_{2,2}(u, v)$	5	14.791	6.431	3.367	1.464	$(2^2 + 3) * (2^2 + 3) = 49$

Note:  $AD$ -Average Distance;  $AvgRE$ -average relative error

**Table 2.** Descriptives of distance and relative error at various decomposition levels ( $N=510$ )

Descriptives of averaged distance (mm)	Decomposition level (control points number)				
	1 (4489)	2 (1225)	3 (361)	4 (121)	5 (49)
Min	0.100	0.134	0.308	0.782	2.792
Max	0.125	0.235	0.622	1.376	3.732
M	0.108	0.170	0.431	1.047	3.212
SD	0.004	0.015	0.044	0.090	0.172
Descriptives of averaged relative error (%)					
Min	0.040	0.057	0.134	0.348	1.210
Max	0.056	0.098	0.254	0.625	1.617
M	0.047	0.074	0.186	0.453	1.389
SD	0.002	0.007	0.019	0.041	0.079

$AD$  and  $AvgRE$  both together reflect the overall approximation of the new surface to the original surface. In this research,  $AD_{j1,j2}$  denotes  $AD$  between the original surface and the low-resolution surface, whose control points' number is  $(2^{j1}+3) \times (2^{j2}+3)$ .

Table 1 shows the approximation errors at various decomposition levels for one sample from our database. The calculation environment is Intel Pentium 4 CPU (2.40GHz), 512MB RAM, and Unigraphics, V18.0. It can be seen that with the recursive decomposition, the number of control points decreases while the approximate errors increase.

The descriptives of  $AD_{j1,j2}$  and  $AvgRE_{j1,j2}$  at various decomposition levels are shown in Table 2. The table shows that the decomposed surfaces can preserve the main shape of the original surface. However, there is a significant increase of the descriptives at level 5 ( $7 \times 7$  poles), which may suggest level 4 as the appropriate decomposition level of head for future data analysis, depending on specific applications and still needs more investigation.

## 5 Conclusions

In this paper, we proposed a multi-resolution pyramid description for 3D anthropometric data, which enables data analysis of 3D anthropometric data progressively in a coarse-to-fine fashion in the wavelet domain. The fundamental properties of wavelets guarantee that the lower dimensionality can preserve the major information and describe the main shape. The multi-resolution description of 3D anthropometric data makes use of not only the coordinates of data points, but also the

geometric characteristics and internal structure among the points. The proposed method in this paper is demonstrated through 510 head data with the aid of a Unigraphics user function. One quantitative approximation error, i.e. MRE, which reflects the approximation of the low-resolution surface to the original one, has been investigated and demonstrated with respect to decomposition levels. Though we only examine head data, which can be used in helmet design, it's also expected to be a helpful universal method for data analysis of other human body surfaces, sizing of shape-fitting wearing items, clinical practice or ergonomically work place design in the future, etc.

**Acknowledgements.** The study is supported by the National Natural Science Foundation of China (No.70571045).

## References

1. Whitestone, J.J.: Design and evaluation of helmet systems using 3D data. In: Proceeding of the Human Factors and Ergonomics Society 37th Annual Meeting. Seattle, USA, 1993, pp. 64–68 (1993)
2. Meunier, P., Tack, D., Ricci, A.: Helmet accommodation analysis using 3D laser scanning. *Applied Ergonomics* 31(4), 361–369 (2000)
3. Wang, M.J., Lin, Y.C., Wu, W.Y.: The development of automated tailoring system using 3D scanning data. In: IEA2003, August 24–29, 2003, Seoul, Korea (2003)
4. Li, Z.Z.: Anthropometric topography. In: Karwowski, W. (ed.) *International Encyclopedia of Ergonomics and Human Factors*, 2nd edn., Taylor & Francis, London (2006)
5. Richtsmeier, J.T., Cheverud, J.M., Lele, S.: Advances in anthropological morphometrics. *Annual Review of Anthropology* 21, 283–305 (1992)
6. Robinette, K.M., Vannier, M.W., Rioux, M., Jones, P.R.M.: 3-D surface anthropometry: review of technologies, agard-ar-329, Dayton Ohio (1997)
7. Robinette, K.M., Blackwell, S., Daanen, H., Fleming, S., Boehmer, M., Brill, T., Hoferlin, D., Burnsides, D.: CAESAR, Final Report, Volume I: Summary. AFRL-HE-WP-TR-2002-0169. United States Air Force Research Lab, Human Effectiveness Directorate, Crew System Interface Division, Dayton Ohio (2002)
8. Bougourd, J., Treleaven, P., Allen, R.M.: The UK national sizing survey using 3d body scanning. In: Eurasia-Tex Conference, Donghua University, Shanghai, China, 2004 (2004)
9. Mochimaru, M., Kouchi, M., Dohi, M.: Analysis of 3-D human foot forms using the free form deformation method and its application in grading shoe lasts. *Ergonomics* 43(9), 1301–1313 (2000)
10. Kouchi, M., Mochimaru, M.: Analysis of 3D human face forms and spectacle frames based on average forms. In: Proceedings of the Digital Human Modeling Conference. Munich, 2002, pp. 69–89 (2002)
11. Paquette, S.: 3D scanning in apparel design and human engineering. *Computer Graphics and Application* 5, 11–15 (1996)
12. Heckbert, P.S.: Multiresolution surface modeling. In: Proceedings of ACM SIGGRAPH 97 (1997)
13. Garland, M.: Multi-resolution modeling: survey and future opportunities. In: Eurographics'99. In: State of The Art Reports of the Annual Conference of the European Association for Computer Graphics, pp. 111–131 (1999)
14. Kobbelt, L., Campagna, S., Vorsatz, J., Seidel, H.P.: Interactive multiresolution modeling on arbitrary meshes. In: Proceedings of ACM SIGGRAPH 98, pp. 105–114 (1998)

15. Hahmann, S., Elber, G.: Constrained multiresolution geometric modeling. In: Dodson, N.A., Sabin, M.A., Floater, M.I. (eds.) *Advances in Multiresolution for Geometric Modeling*, Springer, London (2004)
16. Finkelstein, A., Salesin, D.H.: Multi-resolution curves. In: *Proceedings of the 21st Annual Conference on Computer Graphics and interactive Techniques SIGGRAPH '94*, ACM Press, New York (1994)
17. Farin, G.: *Curves and Surfaces for Computer Aided Geometric Design*, 3rd edn. Academic Press, New York (1992)
18. Farin, G.: *Curves and surfaces for CAGD: a practical guide*. Kaufmann, San Francisco (2002)
19. Hoschek, J., Lasser, D.: *Fundamentals of computer aided geometric design*, 3rd edn. A. K. Peters, Wellesley (1992)
20. Stollnitz, E.J., DeRose, T.D., Salesin, D.H.: Wavelet for computer graphics: a primer. *IEEE Computer Graphics and Applications* 15(3), 76–84 (1995) and 15(4), 75-85 (1995)
21. DeBoor, C.: *A Practical Guide of Splines*, Applied Mathematical Sciences Series, 27 (1978)
22. Chui, C.K.: *An Introduction to Wavelets*. Academic Press, Boston (1992)
23. Quak, E., Weyrich, N.: Decomposition and reconstruction algorithms for spline wavelets on a bounded interval. *Applied and Computational Harmonic Analysis* 1, 217–231 (1994)